Journal of Engineering Science and Technology
Vol. 17, No. 2 (2022) 1078 - 1089

CURCUMIN ADSORPTION ON ZINC IMIDAZOLE FRAMEWORK-8 PARTICLES: ISOTHERM ADSORPTION USING LANGMUIR, FREUNDLICH, TEMKIN, AND DUBININ-RADUSHKEVICH MODELS

RISTI RAGADHITA, ASEP BAYU DANI NANDIYANTO*

Departemen Pendidikan Kimia, Universitas Pendidikan Indonesia
*Corresponding Author: nandiyanto@upi.edu

Abstract

This study aimed to evaluate the suitable isotherm adsorption model of curcumin adsorption onto zinc imidazole framework-8 (ZIF-8) particles. The adsorption was carried out through the batch-experimental method. In this study, prepared ZIF-8 particles and curcumin solution was used as a model of adsorbent and adsorbate, respectively. To support the isotherm adsorption data, suitable isotherm adsorption models (i.e., Langmuir, Freundlich, Temkin, and Dubinin-Radushkevich models) were proposed. In addition to the isotherm adsorption model evaluation, physical characterization was also carried out to characterize the successful preparation of ZIF-8 particles. The scanning electron microscope, Fourier transform infrared, and x-ray diffraction were used to analyse the morphology, functional group, and crystallinity of prepared ZIF-8 particles, respectively. Here, the results of the isotherm adsorption show that the curcumin adsorption is suitable with all isotherm adsorption models and the Langmuir isotherm is most suitable for the adsorption of the curcumin solution onto ZIF-8 particles. The Langmuir adsorption assumes the formation of a monolayer with Van der Waals interactions between the adsorbate-adsorbent.

Keywords: Adsorption isotherm, Batch adsorption, Curcumin, Metal-organic framework.

1. Introduction

Zinc imidazole framework-8 (ZIF-8) is a class of metal-organic framework (MOF) that consists of metal ions and organic linkers/ligands in its structure [1-3]. MOF material is a new material that is being developed since it has unique characteristics including high micropore volume, large pore size, high crystallinity, and high metal content to reach the active site [4]. The larger surface characteristic of the MOF material is a result of its porous structure such as zeolites and activated carbon [5].

The ZIF-8 structure consists of a metal ion that binds to the N atom of a diatomic imidazole ($C_3N_2H_3^-$). Zn^{2+} and Co^{2+} are metals commonly used for the synthesis of ZIF-8. Imidazole as a linker has several types that are commonly suitable used for ZIF-8 synthesis including imidazole (IM), 1-methylimidazole (MIM), 1-ethylimidazole (eIM), and 2-nitroimidazole (nIM) [6]. The different combination of metal ions and linkers is of course correlated with differences in structure and properties. It has been previously mentioned that one of the materials belonging to the MOF class has a porous structure, making them applicable in various fields such as gas sensing, gas storage, and catalysis [7]. ZIF-8 attracts the attention of scientists.

Recently, ZIF-8 has been studied and developed in the field of wastewater treatment as an adsorbent material. ZIF-8 can be used as an adsorbent due to it maintains very well high chemical stability in aqueous environments. Therefore, ZIF-8 is suitable for used to adsorb pollutants in water, dyes, and herbicides. Based on the studies of Majewski et al. [1], Lin and Chang [4], Holopainen et al. [5], Nordin et al. [6], and Lee et al. [7] apart from being chemically stable in water, ZIF-8 material also has a high adsorption capacity. Thus, ZIF-8 is one of the promising candidates for adsorbent material [1, 4-7]. However, to date, only a few studies have been conducted to investigate and evaluate the ability of ZIFs to remove pollutants from water.

Based on our previous studies on the preparation and analysis of metal-organic framework [2, 3], here, we evaluated ZIF's ability isotherm adsorption of ZIF-8 particles. The analysis was supported by several characterizations, including a scanning electron microscope (SEM) instrument, analysis of the presence of functional groups using Fourier Transform Infrared (FTIR) and analysis of the sample phase using X-Ray Diffraction (XRD), as well as UV-Vis spectrophotometers. The analysis of particle size using SEM was done using the same procedure with the previous study [8], and that using XRD analysis was done using the previous literature [9]. The analysis of FTIR was interpreted using a database in literature [10]. The UV-Vis was used for understanding concentration, which was read and interpreted using literature [11]. Then, data from UV-vis was calculated using standard isotherm adsorption, as explained in detail in reference [12].

The ZIF-8 material was specially selected and became an adsorbent model for removing pollutants, especially dyes in water due to the consideration of its porous structure; thus, it can adsorb pollutants.

2. Isotherm Adsorption Models

2.1. Langmuir

The Langmuir isotherm defines the adsorption process in the case of formatting multilayers as well as the monolayer. It depends on whether the adsorption is a physical or chemical process. Four assumptions in the Langmuir isotherm are each

site only adsorbs one adsorbate molecule, molecules are adsorbed by a fixed site, all sites have the same energy, and there is no interaction between the adsorbed molecules and the surrounding sites [13]. Figure 1(a) shows monolayer formation in adsorption. The Langmuir model is expressed by Eq. (1).

$$\frac{1}{Q_e} = \frac{1}{Q_{max} K_L} \frac{1}{C_e} + \frac{1}{Q_{max}} \tag{1}$$

where Q_e is the amount of adsorbed adsorbate molecules per gram of adsorbent (mg/g), Q_{max} is the capacity of the adsorbent monolayer (mg/g), C_e is the adsorbate equilibrium concentration (mg/L), and K_L is the Langmuir adsorption constant referring to the energy of adsorption.

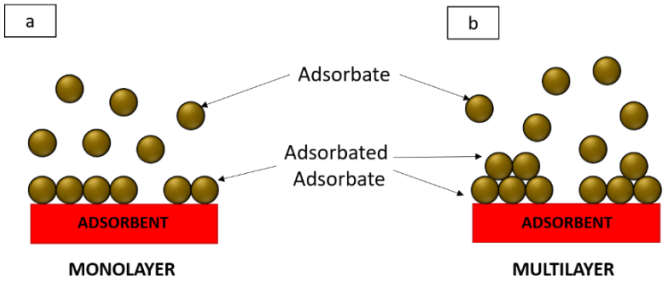

Fig. 1. Illustration of monolayer and multilayer formation.

In the Langmuir isotherm, there is a dimensionless factor or separation factor (R_L) which is described in Eq. (2). R_L parameters are used to support the adsorption process since these parameters are important to analyse each adsorption case separately whether adsorption is favourable or unfavourable. The decrease of R_L value indicating the adsorption process is desirable. In essence, the R_L predicts the affinity between adsorbent and adsorbate.

$$R_L = \frac{1}{1a + K_L C_e} \tag{2}$$

Separation factor (RL) have the following meaning:

(i) $R_L > 1$, unfavourable adsorption (the desorption process is dominant).

(ii) $R_L = 1$, linear adsorption (depending on the amount adsorbed and the concentration adsorbed).

(iii) $R_L = 0$, irreversible adsorption (strong adsorption).

(iv) $0 < R_L < 1$, favourable adsorption (normal adsorption).

2.2. Freundlich

The Freundlich isotherm is based on the assumption that the adsorbent has a heterogeneous surface, and each molecule has different adsorption potentials thus form a multilayer on the adsorbent surface which allows the interaction between adsorbed molecules. The interaction between adsorbed molecules that form a multilayer assumes that the bonds are not strong [14]. Figure 1(b) shows multilayer formation in adsorption. The Freundlich isotherm is defined in Eq. (3).

$$\ln Q_e = \ln k_f + \frac{1}{n} \ln C_e \tag{3}$$

where k_f is the Freundlich constant, C_e is the concentration of adsorbate under equilibrium conditions (mg/L), Q_e is the amount of adsorbate absorbed per unit of adsorbent (mg/g), and n is the value indicating the degree of linearity between the adsorbate solution and the adsorption. The description of the n value is in the following:

(i) $n = 1$, linear adsorption

(ii) $n < 1$, chemisorption process

(iii) $n > 1$, physisorption process

(iv) $0 < 1/n < 1$, favourable adsorption

(v) $1/n > 1$, cooperative adsorption

2.3. Temkin

The Temkin isotherm assumes the correlation of the indirect adsorbate interaction with the isotherm adsorption. The adsorption heat of all the molecules decreases linearly with increased adsorbent coverage surface, and adsorption is characterized by a uniform distribution of the binding energy [15]. The Temkin isotherm can be explained by Eq. (4).

$$q_e = B_T \ln A_T + B_T \ln C_e \tag{4}$$

where B_T is the adsorption heat constant (if the B_T value is less than 8 kJ/mol, then the adsorption occurs physically), A_T is the binding equilibrium constant, and T is the absolute temperature.

2.4. Dubinin-Radushkevich

The Dubinin-Radushkevich isotherm assumes the size of the adsorbent is in the micrometre range. The adsorption equilibrium relationship for the adsorbents is independently expressed from temperature using the adsorption potential (ε). The Dubinin-Radushkevich adsorption equilibrium model shows that adsorption following the pores' filling mechanism is not a layer-by-layer form [16]. The Dubinin-Radushkevich is described by Eq. (5).

$$\ln q_e = \ln q_s - (\beta \varepsilon^2) \tag{5}$$

where β is the Dubinin-Radushkevich isotherm constant, q_s refers to the saturation capacity of theoretical isotherms, and $\mathcal{E}$ is the Polanyi potential (J/mol) is determined using Eq. (6).

$$\varepsilon = RT \ln \left[1 + \frac{1}{C_e}\right] \tag{6}$$

Adsorption free energy per adsorbate molecule is calculated using Eq. (7).

$$E = \frac{1}{\sqrt{2\beta}} \tag{7}$$

where C_e is the final concentration of solute and E is the adsorbate energy per molecule as the energy needed to remove molecules from the surface. Adsorbate energy per molecule has the following value:

(i) If $E < 8$ kJ/mol describes physisorption process.

(ii) If $8 < E < 168$ kJ/mol describes chemisorption process.

Efficiency adsorption (E) was calculated using Eq. (8).

$$\%E = \left(\frac{C_o - C_e}{C_o}\right) \times 100\% \quad (8)$$

3.Method

3.1. Materials

Some of the main raw materials for the synthesis of ZIF-8 particles, including Zinc nitrate ($Zn(NO_3)_2.6H_2O$) and 2-Methyl Imidazole (MIM) as precursor and methanol as a solvent.

3.2. Method

In this study, ZIF-8 particles were synthesized via an aqueous synthesis route. Zinc nitrate and 2-MIM precursors with appropriate composition were dissolved in methanol solution in a separate container. After each of the precursors in the different containers was completely dissolved in methanol, the two precursors were mixed to form a dissolved solution mixture. After that, the mixture solution was stirred for 8 hours at room temperature until the solution turned white which was originally a colourless mixture of solutions. The white discoloration of the solution occurs due to the formation of a solid suspension of ZIF-8 particles. At this stage, the ZIF-8 particles were successfully synthesized. Then, the solution mixture was centrifuged and filtered to separate the filtrate and ZIF-8 particles. The collected ZIF-8 particles were then dried using an oven under 50°C for 1 hour to evaporate the remaining methanol solvent. The illustration of ZIF-8 particle synthesis is shown in Fig. 2.

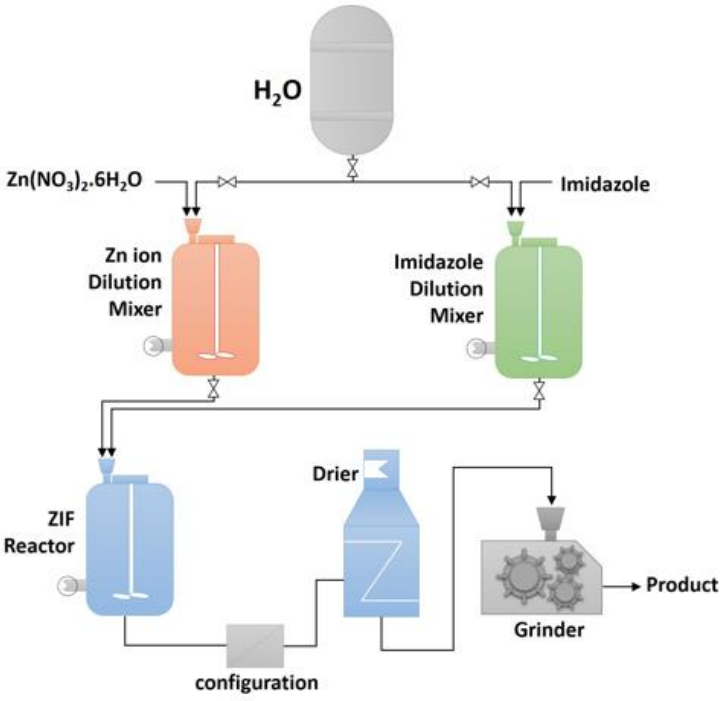

Fig. 2. Illustration process of ZIF-8 particles synthesis adopted from [3].

3.3. Physical characterization of ZIF-8 particles

Several characterizations to confirm the success of ZIF-8 synthesis have been carried out, including analysis of the morphological structure of the sample using the SEM, analysis of the presence of functional groups using the FTIR (FTIR-4600, Jasco Corp, Japan), and analysis of the sample phase using XRD (PANalytical X'Pert PRO; Philips Corp., The Netherland). The analysis of particle size using SEM was done using the same procedure with the previous study [8], and that using XRD analysis was done using the previous literature [9]. The analysis of FTIR was interpreted using a database in literature [10].

3.4. Adsorption experiments

Isotherm adsorption was carried out through batch method in 500 mL-borosilicate glass. The adsorption is carried out by mixing a certain number of ZIF-8 particles as adsorbent into 200 mL-curcumin solutions with a certain concentration (i.e., 20, 40, 60, and 80 ppm) under the stirring condition of 1000 rpm for 1 hour at constant pH, temperature, and pressure. We chose a rotation speed of 1000 rpm due to if the rotation speed is too slow, the ZIF-8 particles easily settle and cause the ZIF-8 particles not to be dispersed in the adsorbate thus the contact between the adsorbent and the adsorbate is relatively weak. Although we know, the drawback is that if the rotation speed is too fast it will cause desorption.

Curcumin was prepared by extracting turmeric (Curcuma Longa; obtained from the local market in Bandung, Indonesia) as our previous study [17]. The curcumin solution was chosen as the adsorbate model because it has the ideal molecular size as an organic molecule and for safety purposes. After all, many organic molecules, especially those used as dye models, have toxic characteristics [17].

Before analysing the concentration of curcumin, curcumin solution was centrifuged and filtered to separate filtrate solution with adsorbent. After that, 2 mL-curcumin solution filtrate was analyse using UV-VIS spectrophotometer (Model 705; JENWAY; Cole-Parner; US) at a wavelength of 280-500 nm to measure the absorbance of the curcumin solution.

The absorbance of the curcumin solution was plotting, normalizing, and calculating based on Lambert-Beer analysis. The UV-Vis was used for understanding concentration, which was read and interpreted using literature [11].

Then, data from UV-vis was calculated using standard isotherm adsorption, as explained in detail in reference [12]. The data obtained were then plotted and compared with standards adsorption isotherm models: Langmuir, Freundlich, Temkin, and Dubinin-Radushkevich model.

4. Results and Discussion

4.1. Physical characterizations

Figures 3(a) and (b) show the results of the characterization of ZIF-8 particles using a scanning electron microscope with magnifications of 1000 (a) and 2000x (b). Based on the SEM result, the ZIF-8 particles that have been prepared have a hexagonal morphology, agglomeration, and inhomogeneous particle size.

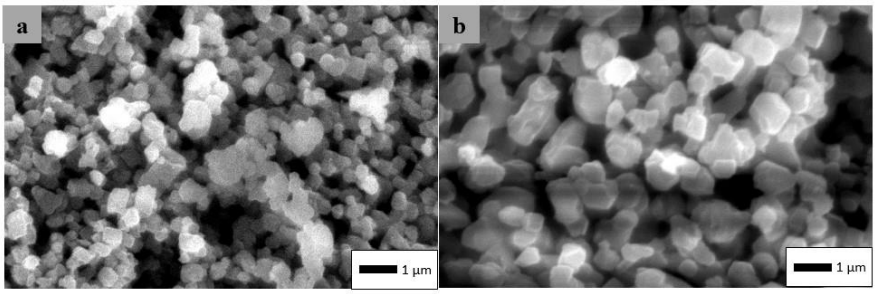

Fig. 3. SEM images of prepared ZIF-8 particles.

Figure 4 shows FTIR spectra of ZIF-8 particles. The peak characteristic in the area of 1590 cm^{-1} shows a vibration of C=N stretching. The absorption band in the area between 1300-1500 cm^{-1} is the whole stretching of the ring structure. The existence of the Zn-N bond is shown in the vibration region of 450 cm^{-1} [12, 18, 19].

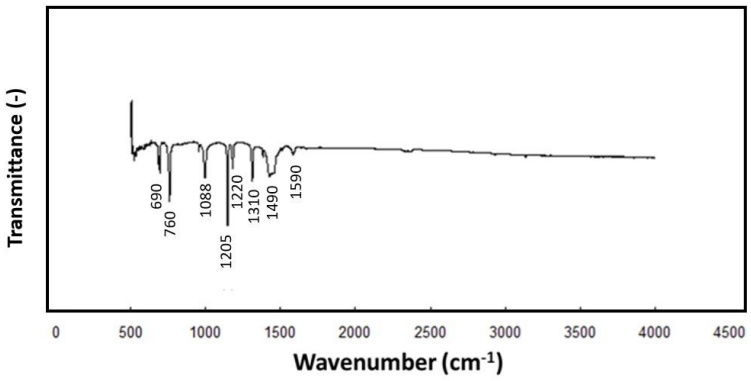

Fig. 4. FTIR spectra of prepared ZIF-8 particles.

Figure 5 shows diffraction patterns of ZIF-8 particles. Based on the results of XRD spectra, ZIF-8 particles have high intensity and sharp peaks. The sharp peak intensity indicates that the product is pure in the crystalline phase. It means ZIF-8 particles have a good crystallinity structure. The peaks that indicate the success of the synthesis of ZIF-8 particles are indicated by the presence of main peaks in the regions 2θ = 7.30; 10.35; 12.00; and 18.35, respectively [6, 15, 20]. The results showed that the pure ZIF phase formation was successfully carried out in this study.

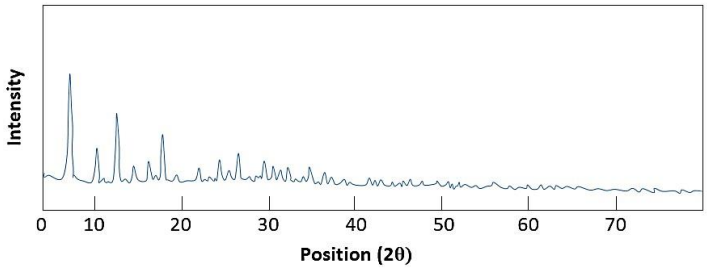

Fig. 5. XRD peal of prepared ZIF-8 particles.

4.2. Curcumin adsorption onto ZIF-8 particles

Figure 6 shows isotherm adsorption of prepared ZIF-8 particles. Table 1 shows parameter values of all model isotherm adsorptions. Isotherm adsorption analysis was performed to determine the characteristics and possible mechanisms of particular adsorption [12]. After fitting the data to the isotherm adsorption model, overall, the adsorption results from the ZIF-8 particles prepared is suitable with all isotherm model due to the correlation coefficient is relatively high ($R^2 > 0.80$). Here, the most suitable adsorption model is the Langmuir isotherm. This compatibility is known from the value of the highest correlation coefficient (0.959) for Langmuir isotherm (see Table 1). Based on Table 1, the suitability of the adsorption isotherm if sorted consecutively is Langmuir > Freundlich > D-R > Temkin. The detailed description for each model is discussed as follows.

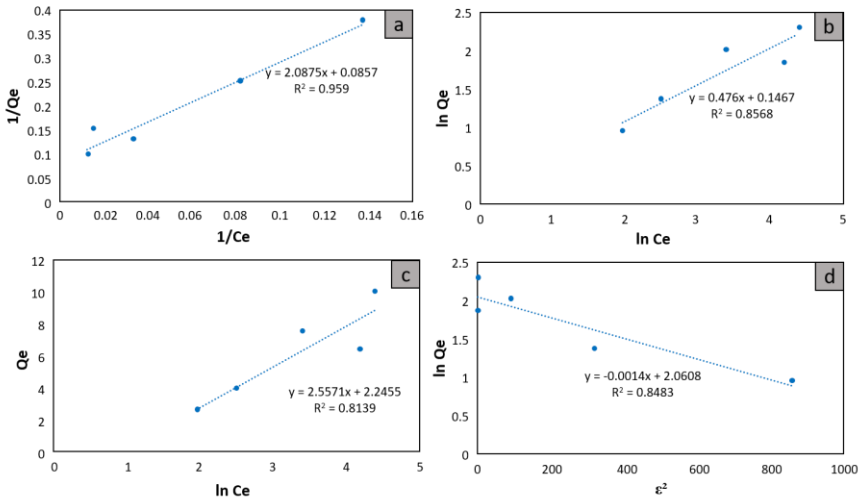

Fig. 6. Isotherm adsorption (a) Langmuir, (b) Freundlich, (c) Temkin, and (d) Dubinin-Radushkevich of prepared ZIF-8 particles.

The Langmuir isotherm (see Figure 6(a)) is the most suitable isotherm model in this study compared to other isotherm models. Equations (1) and (2) were used to analyse Langmuir adsorption parameters such as q_{max}, K_L, R_L, and R^2. The results of the Langmuir parameter are shown in Table 1. The Langmuir isotherm assumes that the adsorption occurs on the surface of the monolayer adsorbent and there is no interaction for each adsorbate molecule adsorbed. Monolayer adsorption occurs due to the weak adsorbate-adsorbent interaction which is shown by the K_L value. Based on the Langmuir parameter value, adsorption allows favourable adsorption due to the R_L value is in the range $0 < R_L < 1$.

The Freundlich isotherm (see Figure 6(b)) is the second most suitable isotherm model. The Freundlich parameter that has been analysed shows the unique characteristics of the adsorption such as the values of K_f, n, $1/n$, and R^2. The Freundlich parameter was calculated using Eq. (3). Based on $1/n$ parameter ($0 < 1/n < 1$), adsorption is favourable adsorption in the heterogeneous surface. It means adsorption occurs normally adsorption with the physisorption process.

The Temkin isotherm (see Figure 6(c)) was studied using Eq. (4) to determine the parameters of A_T, B_T, and R^2. The Temkin isotherm assumes that the heat of adsorption decreases linearly if the bonding energies are uniformly distributed. The Temkin isotherm model is the third model that is also suitable for curcumin adsorption onto ZIF particles. Based on the Temkin isotherm, adsorption energy confirming the physisorption process due to its value of $E < 8$ kJ/mol.

The fitting curve of the Dubinin-Radushkevich adsorption isotherm (see Figure 6(d)) was analysed to determine the Dubinin-Radushkevich parameters such as the values of q_s, E, and R^2 using Eq. (5). Based on the Dubinin-Radushkevich isotherm, adsorption allows a physisorption process on the surface of the adsorbent.

Table 1. Parameter of isotherm adsorption.

Model	Parameter	Value	Note
Langmuir	Q_{max} (mg/g)	11.668	Adsorbent capacity.
	K_L (L/mg)	0.049	Weak interaction adsorbate-adsorbent due to the adsorption energy (K_L value) is relatively small.
	R_L	0.289	$0 < R_L < 1$ describes favourable adsorption.
	R^2	0.959	The correlation coefficient.
Freundlich	K_F (mg/g)	1.650	The adsorption capacity of the adsorbent.
	$1/n$	0.402	$0 < 1/n < 1$ indicates favourable adsorption that occurs in heterogenous adsorbent surface.
	n	2.589	$n > 1$ explains physisorption process.
	R^2	0.8568	The correlation coefficient.
Temkin	A_T (L/g)	1.0023	Temkin equilibrium binding constant.
	B_T (J/mol)	957	$B_T <$ kJ/mol indicates physisorption process.
	R^2	0.8139	The correlation coefficient.
Dubinin-Radushkevich	Qs (mg/g)	1.406	Capacity adsorption of adsorbent.
	B (mol^2/kJ^2)	-0.0014	D-R constant.
	E (kJ/mol)	27.027	$E < 8$ kJ/mol indicates physisorption.
	R^2	0.8483	The correlation coefficient.

Based on isotherm adsorption, The adsorption of curcumin solution onto the ZIF-8 particles is predicted to follow the Langmuir isotherm with the following assumptions: (a) the adsorption occurs on a homogeneous surface, allowing the formation of a monolayer on the adsorbent surface; (b) no adsorbate-adsorbent interactions; as well as (c) each site energy that adsorbs the adsorbate molecule has

uniform energy [13] and based on Eq. (8), the adsorption efficiency of curcumin adsorption onto ZIF-8 particles is 25%.

Apart from the analysis based on the Langmuir isotherm, other adsorption isotherms such as Freundlich, Temkin, and D-R were also considered. Based on Freundlich, Temkin, and Dubinin-Radushkevich isotherms, the adsorption of curcumin molecules onto ZIF-8 adsorbent shows physical process adsorption. Physical adsorption occurs when the intermolecular force is greater than the force attraction between molecules or relatively weak attractive forces between adsorbate with the adsorbent surface [21]. This force is called the Van der force Waals thus the adsorbate had abilities to move from one part of the surface to the other surface parts of the adsorbent.

In addition to the presence of monolayer adsorption, Freundlich isotherm also confirms the presence of multilayer adsorption, this is probably due to the pore structure of the ZIF adsorbent [22, 23]. The existence of a porous structure must exist confirmed by further analyses such as nitrogen uptake analysis, which will be carried out in our future work. In this case, we proposed the adsorption mechanism as we can see in Fig. 7.

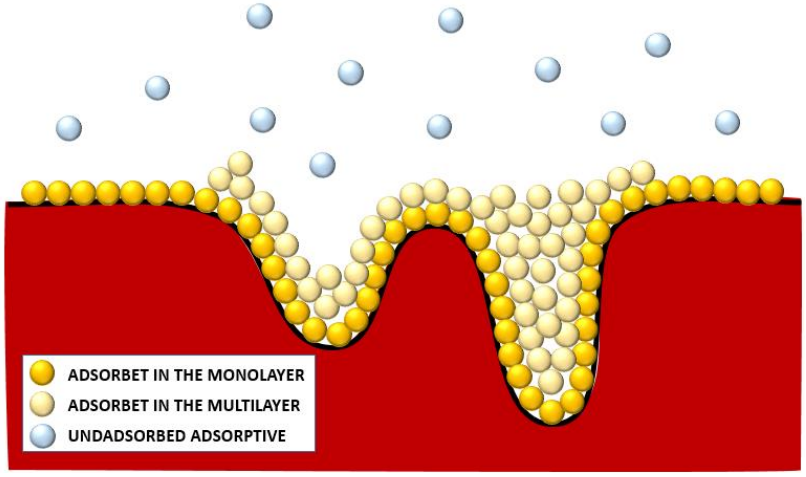

Fig. 7. The proposed adsorption mechanism [12].

In addition, the use of filtration before the analysis part may cause inaccurate results because a significant amount of curcumin dye adheres to the filtration paper. A sufficient time for separating layers is more appropriated. However, our research has a weakness because too small particles are easily dispersed in the adsorbate even though they have been separated by a centrifugation method and it will still interfere with the concentration calculation in UV-VIS spectroscopy. Therefore, even though the adsorbate and adsorbent have been separated by means of the centrifugation method, they must still be separated manually.

5. Conclusion

Evaluation of the curcumin adsorption onto ZIF-8 adsorbent particles has been successfully evaluated. The adsorption results show that the adsorption of curcumin

onto ZIF-8 particles shows compatibility with the Langmuir model which assumes that the adsorption occurs by forming a monolayer on the adsorbent surface. Physical adsorption characterizes the adsorption in this case. Physical adsorption is adsorption that occurs because of the Van Der Waals force (relatively weak attractive force) between the adsorbate and the adsorbent surface. The pore structure of the ZIF particles provides additional adsorption by forming a multilayer structure on the adsorbent surface.

Acknowledgements

We acknowledged Ristek Brin, grant Penelitian Unggulan Perguruan Tinggi, and Bangdos, Universitas Pendidikan Indonesia.

References

1. Majewski, M.B.; Peters, A.W.; Wasielewski, M.R.; Hupp, J.T.; and Farha, O.K. (2018). Metal-organic frameworks as platform materials for solar fuels catalysis. *ACS Energy Letters*, 3(3), 598-611.
2. Ragadhita, R.; and Nandiyanto, A.B.D. (2020). Concentrations of metal ions and ligands on the formation of nano to submicron zinc imidazole Framework-8 particles. *Journal of Engineering Science and Technology* (*JESTEC*), 15(1), 364-371.
3. Nandiyanto, A.B.D.; and Ragadhita, R. (2019). Feasibility study in the production of zinc imidazole framework particles. *Journal of Engineering Research*, 7, 36-49.
4. Li, Z.; Zhang, J.W.; Yu, L.G.; and Zhang, J.W. (2017). Electrospun porous nanofibers for electrochemical energy storage. *Journal of Materials Science*, 52(11), 6173-6195.
5. Holopainen, J.; Heikkilä, M.J.; Salmi, L.D.; Ainassaari, K.; and Ritala, M. (2018). Zeolitic imidazole Framework-8 (ZIF-8) fibers by gas-phase conversion of electroblown zinc oxide and aluminum-doped zinc oxide fibers. *Microporous and Mesoporous Materials*, 267, 212-220.
6. Nordin, N.A.H.M.; Ismail, A.F.; Mustafa, A.; Goh, P.S.; Rana, D.; and Matsuura, T. (2014). Aqueous room temperature synthesis of zeolitic imidazole framework 8 (ZIF-8) with various concentrations of triethylamine. *RSC advances*, 4(63), 33292-33300.
7. Lee, J.; Farha, O.K.; Roberts, J.; Scheidt, K.A.; Nguyen, S.T.; and Hupp, J.T. (2009). Metal–organic framework materials as catalysts. *Chemical Society Reviews*, 38(5), 1450-1459.
8. Yolanda, Y. D.; and Nandiyanto, A. B. D. (2022). How to read and calculate diameter size from electron microscopy images. *ASEAN Journal of Science and Engineering Education*, 2(1), 11-36.
9. Fatimah, S.; Ragadhita, R.; Al Husaeni, D. F.; and Nandiyanto, A. B. D. (2022). How to calculate crystallite size from X-ray diffraction (XRD) using scherrer method. *ASEAN Journal of Science and Engineering*, 2(1), 65-76.
10. Nandiyanto, A. B. D.; Oktiani, R.; and Ragadhita, R. (2019). How to read and interpret FTIR spectroscope of organic material. *Indonesian Journal of Science and Technology*, 4(1), 97-118.

11. Pratiwi, R. A.; and Nandiyanto, A. B. D. How to Read and Interpret UV-VIS spectrophotometric results in determining the structure of chemical compounds. *Indonesian Journal of Educational Research and Technology*, 2(1), 1-20.
12. Ragadhita, R.; and Nandiyanto, A.B.D. How to calculate adsorption isotherms of particles using two-parameter monolayer adsorption models and equations. *Indonesian Journal of Science and Technology*, 6(1), 205-234.
13. Langmuir, I. (1918). The adsorption of gases on plane surfaces of glass, mica and platinum. *Journal of the American Chemical Society*, 40(9), 1361-1403.
14. Tan, I.A.W.; Chan, J.C.; Hameed, B.H.; and Lim, L.L.P. (2016). Adsorption behavior of cadmium ions onto phosphoric acid-impregnated microwave-induced mesoporous activated carbon. *Journal of Water Process Engineering*, 14, 60-70.
15. Voudrias, E.; Fytianos, K.; and Bozani, E. (2002). Sorption–desorption isotherms of dyes from aqueous solutions and wastewaters with different sorbent materials. *Global Nest International Journal*, 4(1), 75-83.
16. Günay, A.; Arslankaya, E.; and Tosun, I. (2007). Lead removal from aqueous solution by natural and pretreated clinoptilolite: adsorption equilibrium and kinetics. *Journal of Hazardous Materials*, 146, 362-371.
17. Ragadhita, R.; Nandiyanto, A.B.D.; Nugraha, W.C.; and Mudzakir, A. (2019). Adsorption isotherm of mesopore-free submicron silica particles from rice husk. *Journal of Engineering Science and Technology* (*JESTEC*), 14(4), 2052-2062.
18. Hu, Y.; Kazemian, H.; Rohani, S.; Huang, Y.; and Song, Y. (2011). In situ high pressure study of ZIF-8 by FTIR spectroscopy. *Chemical Communications*, 47, 12694-12696.
19. He, M.; Yao, J.; Liu, Q.; Wang, K.; Chen, F.; and Wang, H. (2014). Facile synthesis of zeolitic imidazolate framework-8 from a concentrated aqueous solution. *Microporous and Mesoporous Materials*, 184, 55-60.
20. Yao, J.; Chen, R.; Wang, K.; and Wang, H. (2013). Direct synthesis of zeolitic imidazolate framework-8/chitosan composites in chitosan hydrogels. *Microporous and Mesoporous Materials*, 165, 200-204.
21. Al-Degs, Y.S.; El-Barghouthi, M.I.; El-Sheikh, A.H.; and Walker, G.M. (2008). Effect of solution pH, ionic strength, and temperature on adsorption behavior of reactive dyes on activated carbon. *Dyes and Pigments*, 77(1), 16-23.
22. Nandiyanto, A.B.D.; Girsang, G.C.S.; Maryanti, R.; Ragadhita, R.; Anggraeni, S.; Fauzi, F.M.; and Al-Obaidi, A.S.M. (2020). Isotherm adsorption characteristics of carbon microparticles prepared from pineapple peel waste. *Communications in Science and Technology*, 5(1), 31-39.
23. Fiandini, M.; Ragadhita, R.; Nandiyanto, A.B.D.; and Nugraha, W. C. (2020). Adsorption characteristics of submicron porous carbon particles prepared from rice husk. *Journal of Engineering Science and Technology* (*JESTEC*), 15, 022-031.